

Influence of Residual Stresses on the Mechanical Properties of a Layered Ceramic Composite

O. Sbaizero & E. Lucchini

Dipartimento di Ingegneria dei Materiali e Chimica Applicata, Università di Trieste, Via Valerio — 34127 Trieste, Italy

(Received 7 June 1995; revised version received 6 December 1995; accepted 12 December 1995)

Abstract

A layered Al_2O_3 – ZrO_2 ceramic composite has been fabricated using a colloidal processing method. The technique uses sequential centrifuging of slurries containing suspended ceramic powders to form a three-layered structure. The outer layers have a high alumina content while the central layer contains mainly stabilized zirconia. These laminae are subjected to residual stresses due to their different thermal expansion coefficients. These stresses depend on the configuration of the system as well as on the amount of the zirconia in the two layers.

If the residual stresses exceed the strength of the inner layer, periodic parallel cracks are produced. Such cracks of course adversely influence the structural performance of the composite and should be avoided. A model for this problem is presented.

Vickers indentations were also placed into the tensile layer with the intent to explore the crack propagation in such system. Cracks were split after they reached the compressive layer. The effects of the layer thickness on the depth of the cracks beneath the interface were systematically explored.

1 Introduction

The majority of attention in the production of reliable ceramics for structural applications has been paid to either the development of stronger materials through processing and microstructural refinements, in order to minimize the flaw size or in the activation of an *R*-curve behaviour introducing toughening mechanisms using platelets, whiskers or fibres to reinforce ceramic matrices.^{1–7}

Concerns about both methods include the correct choice of the components, their availability and price as well as the processing cost. It is in fact difficult to imagine the market competitiveness of

ceramics with a very high price. Besides, there are applications in which structural ceramics must exhibit above all high strength and hardness combined with some degree of resistance to damage introduced in service.

A well recognised and inexpensive method of achieving the aforementioned results is the introduction of surface compressive stress, an approach normally used in glasses.^{8,9} In the ceramics this goal can be obtained through the production of laminate ceramic composites^{10–14} using the build-up of residual stresses due to the thermal expansion mismatch between the different layers to enhance the mechanical properties.

The variable ‘layer composition’ as well as the system’s geometry allows the designer to control the magnitude of the residual stresses in such a way that compressive stresses, in the outer layers near the surface, increase strength, hardness, flaw tolerance and probably also fatigue strength and stress corrosion cracking.

During this investigation a three-layered structure has been fabricated using colloidal techniques^{1–5} combined with sequential centrifuging of the slurries to consolidate the layers.

The outer layers are made of alumina containing different amounts of zirconia while the inner layer contains mainly zirconia with a small amount of alumina. This system was selected because both oxides are mutually insoluble, there are no intermediate phases and pressureless sintering produces materials with near theoretical density. At high temperature, all stresses relax due to thermally activated processes. During cooling, the alumina rich layers contract less than the zirconia rich inner layer, since the outer layers’ thermal dilatation is lower. As a consequence there will be a distribution of tensile and compressive residual stresses. A symmetrical layered material, with zirconia as the inner layer, is therefore expected to exhibit the desired compressive stress near the surface. If the system geometry is maintained constant, the residual

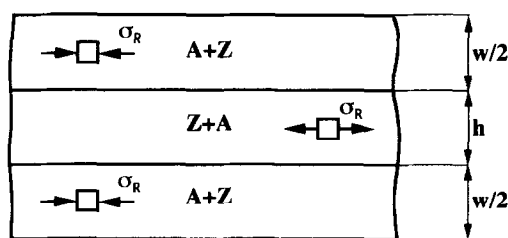


Fig. 1. Schematic of an ideal layered material.

stress depends on the composition, in any case the inner layer is under tensile residual stress while the outer layers are subjected to compressive stresses. Figure 1 shows a schematic of an ideal specimen. The magnitude of these stresses can also be tailored by varying the $\text{Al}_2\text{O}_3/\text{ZrO}_2$ ratio in the layers.

The aim of the present study is to characterize the mechanical properties of a trilayer laminate composite as well as to compare crack path predictions with experimental observations.

2 Experimental Procedure

The layers were produced starting from aqueous slurries containing 25 vol% powders: α -alumina (Sumitomo Chemical Co. AKP-20) and zirconia+3 mol% yttria (Dynamit Nobel); these powders were chosen because their particles have comparable sizes. The slurries were prepared by dispersing the powders with a blender (6000 rpm) in deionized water. The pH values of the dense slurries were adjusted to ≈ 4 using HNO_3 (1 M) to provide large electrostatic repulsive forces between the particles, the slurry was also ultrasonically homogenized for 3 min at 300 W in order to break down the aggregates. After ultrasonication, slurries were equilibrated for 4 h in a planetary mixer and then NH_4NO_3 was added to induce strong short range repulsive forces between the particles. The slurry in this situation is called 'coagulated'¹⁵ and the short range repulsive potential is able to induce a weakly attractive particle network that allows particles to pack to a high relative density by centrifugation preventing also mass segregation.

Quantities of slurries enough to yield the desired thickness of layer were placed in a Teflon cylindrical container (diameter = 50 mm) and were centrifuged for 60 min at 2000g. After that the supernatant liquid was poured off, another volume of suspension, containing a solid phase with different composition, was placed in the container in order to deposit the next layer. This procedure was repeated until multilaminar composites with layer thickness ranging from 0.1 to 0.3 mm

were obtained. Consolidated bodies were air dried for 24 h at 65°C and then cold isostatically pressed at 100 MPa. The disk-shaped samples were heated from room temperature to 200°C over a 3 h period, after which the temperature was raised to 1550°C at 10°C/min and ultimately held at this temperature for 3 h after which it was lowered to room temperature over the next 4 h.

The bending strength at room temperature was measured with a universal testing machine, using a 4-point bending with outer and inner span of 40 and 20 mm respectively and a crosshead speed of 0.01 mm/min on $4 \times 3 \times 45$ mm bars cut from the disk-shaped samples produced by centrifuging. These tests were also carried out on samples with different outer/inner layer thickness with the total thickness remaining constant in order to assess the influence of the stress magnitude on the total strength.

The assessment of the residual stresses requires knowledge of Young's modulus, Poisson's ratio and the thermal expansion coefficient for the single layers; the former two data were derived from the longitudinal and shear ultrasonic wave velocities, the latter with a dilatometer up to 1450°C.

Vickers indentations were used to assess the hardness and also when placed into the central layer to explore the crack propagation in such systems. Residual stresses were also emphasized placing Vickers indentations in the different layers. Polished sections of the samples were examined before and after thermal etching. Secondary electron and back scattered images were obtained in a scanning electron microscope.

3 Results

As far as the microstructure is concerned, in bodies produced with coagulated slurries, Al_2O_3 and ZrO_2 were observed to be uniformly mixed, see Fig. 2. Another observation is that thermal expansion mismatch sometimes produced periodic parallel cracks in the inner layer, see Fig. 3. Such cracks of course adversely influence the structural performance of the composite and should be avoided.

As far as the indentations are concerned, the compressive stress in the outer layers reduces the crack propagation toward the interface with the tensile layer, see Fig. 4, whereas if enough load (> 60 kg) was applied in the inner layer, a crack propagated through it, but after reaching the interface with the layer in compression it bifurcates, see Fig. 5.

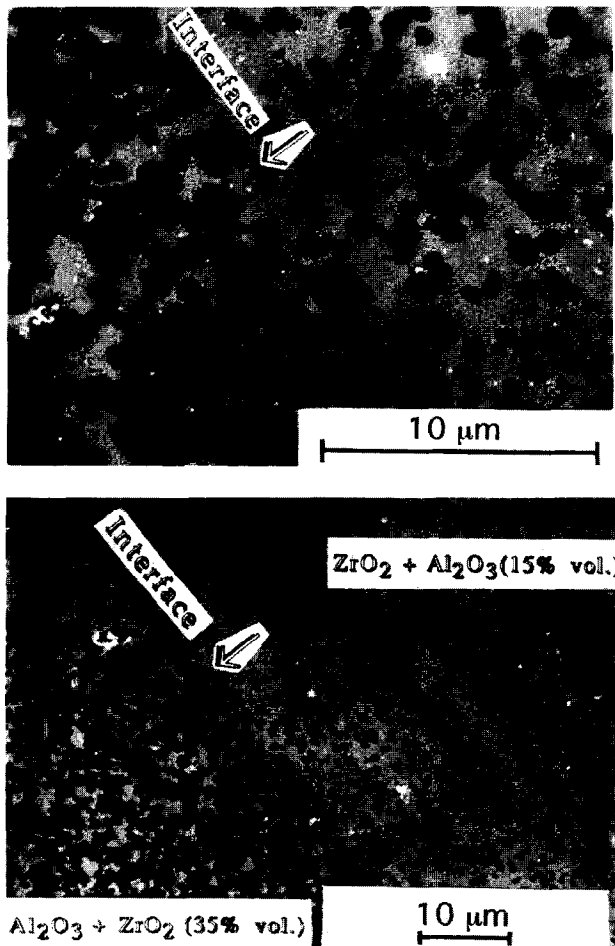


Fig. 2. Backscattered images of an interface between two layers of different composition.

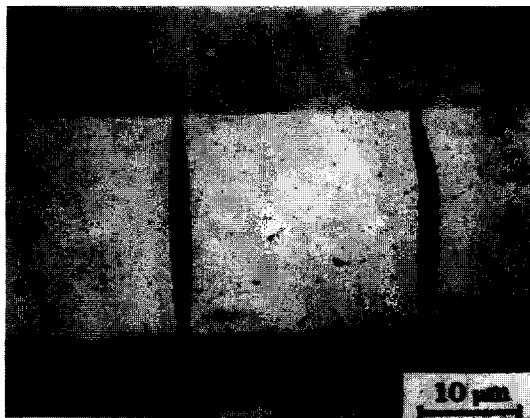


Fig. 3. Periodic cracks developed in an inner layer due to residual stress.

4 Discussion

4.1 Matrix cracking

The residual thermal stress in a layer bonded between two identical substrates (Fig. 1) is biaxial, with the magnitude:¹⁶

$$\sigma_R = \frac{\epsilon_R E_i}{1 - \nu_i} \left[1 + \frac{h E_i / (1 - \nu_i)}{w E_o / (1 - \nu_o)} \right]^{-1} \quad (1)$$

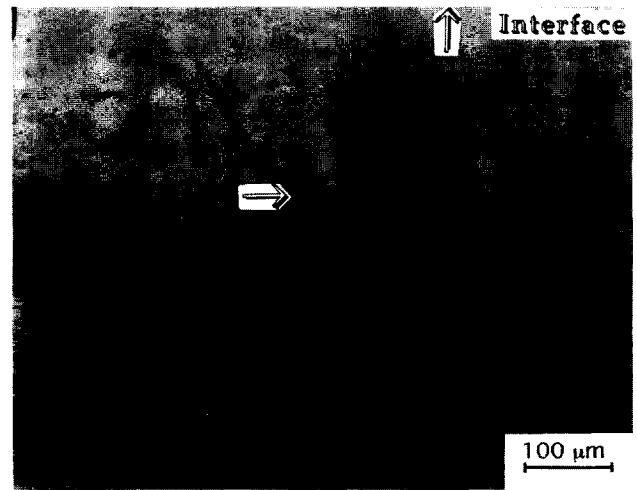


Fig. 4. Vickers indentation in an inner layer.



Fig. 5. Crack bifurcation during the propagation in outer layer.

where ν is Poisson's ratio, E is Young's modulus, h the thickness of the inner layer and $w/2$ the thickness of each outer layer, the subscripts o and i distinguish the outer and inner layer respectively.

ϵ_R is the thermal mismatch strain and is given by:

$$\epsilon_R = \int_T^{T_0} (\alpha_i - \alpha_o) dT \quad (2)$$

where T_0 and T are the processing and the current temperature and α is the thermal expansion coefficient. The two outer layer thickness being the

same, the stressed sandwich remains flat, so that the residual stresses are difficult to detect. When these residual stresses, in the layer under tension, exceed the strength of the material, transverse cracks start to develop.

Previous investigations¹⁷⁻²⁰ have recognized that a critical non-dimensional group of parameters \mathcal{R} exists, below which cracking does not occur. \mathcal{R} is defined as:

$$\mathcal{R} = R (E_m \Delta\alpha \Delta T / K_m)^2 \quad (3)$$

Where R is the reinforcement size, E_m the Young's modulus matrix, $\Delta\alpha$ the thermal expansion mismatch, ΔT the processing temperature range and K_m the matrix toughness. The significance of this coefficient is that cracking, in the matrix under tension, is found to be suppressed when \mathcal{R} is less than a critical value, \mathcal{R}_c . The magnitude of the cracking coefficient, \mathcal{R}_c , depends on the volume fraction of the reinforcement as well as the elastic modulus and Poisson's ratio between reinforcement and matrix.

The model has been developed for cracking around elastic inclusions²¹ but it has been used also for ceramic matrix composites containing elastic reinforcements²² with periodic parallel cracks normal to the fibre axis; the present study might extend the aforementioned results for ceramic composites, to include also sandwich structures. In this case the 'matrix' will be the inner layer whereas the 'reinforcements' will be the outer layers, therefore \mathcal{R} is given by:

$$\mathcal{R} = (w/2) (E_i \Delta\alpha \Delta T / K_i)^2 \quad (4)$$

where $(w/2)$ is the outer layer thickness, E_i the inner layer Young's modulus, K_i the outer layer toughness, $\Delta\alpha$ and ΔT being, as before, the processing temperature range and the difference in thermal expansion coefficient.

For a well-bonded interface \mathcal{R}_c has the form:²¹

$$\mathcal{R}_c = \sqrt{6} B^2 (1 - \nu)^3 (1 + \nu)^{1/2} / f(1 - f) \quad (5)$$

where B is a coefficient between 0.8 and 1, f is the volume fraction of the reinforcement. The trend for \mathcal{R}_c in the case of a well bonded interface and with $B=0.8$ is plotted in Fig. 6. The two dashed lines highlight the sample geometry used in this study. Transverse cracks are found to be suppressed provided that $\mathcal{R} < 3-4$, whereas profuse cracking should be expected when $\mathcal{R} > 5$.

In order to compare the results of our observations with the calculations we focused our attention on several compositions. For every one we assessed the thermal expansion coefficient as well as Young's modulus and toughness. Results are reported in Table 1. Keeping constant the inner layer composition (either $\text{ZrO}_2 + 15\% \text{Al}_2\text{O}_3$ or

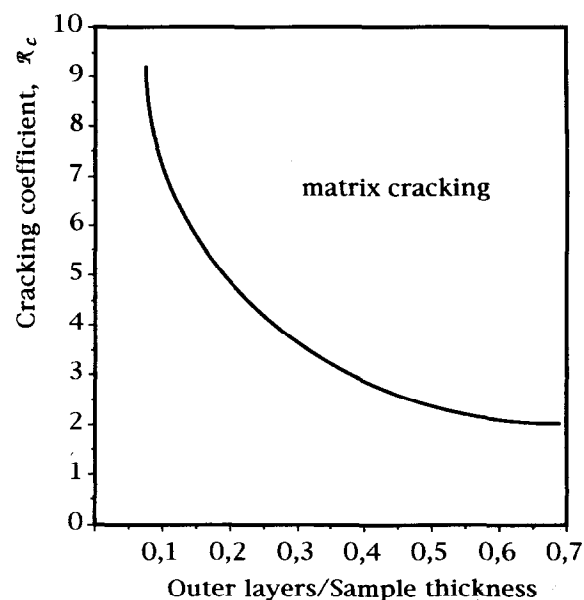


Fig. 6. Trend in the cracking coefficient, \mathcal{R}_c with inner layer/sample thickness ratio for materials with well-bonded interfaces.

Table 1. Experimental results for the formation of the periodic parallel cracks in the tensile layer

Outer layer composition	α (10^{-6}K^{-1})	\mathcal{R}	Observation
Alumina	8.4	31	Cracks
A+20%Z	9.58	8.6	Cracks
A+35%Z	9.8	6	Cracks
A+50%Z	10.25	2	No cracks
A+70%Z	10.5	0.8	No cracks

Inner layer composition: $\text{ZrO}_2 + 15\% \text{Al}_2\text{O}_3$, ($E = 222 \text{ MPa}$, $\alpha = 10.9 \times 10^{-6} \text{K}^{-1}$, $K_{Ic} = 4.9 \text{ MPa } \sqrt{\text{m}}$, $\Delta T = 1550^\circ\text{C}$).

Outer layer thickness = $2000 \mu\text{m}$. Outer layer/sample thickness = 0.3.

Outer layer composition	α (10^{-6}K^{-1})	\mathcal{R}	Observation
Alumina	8.4	32	Cracks
A+20%Z	9.58	5.4	Cracks
A+30%Z	9.75	3.4	Cracks
A+40%Z	10	1.3	No cracks
A+50%Z	10.25	0.18	No cracks
A+70%Z	10.5	0.08	No cracks

Inner layer composition: $\text{ZrO}_2 + 35\% \text{Al}_2\text{O}_3$, ($E = 260 \text{ MPa}$, $\alpha = 10.4 \times 10^{-6} \text{K}^{-1}$, $K_{Ic} = 4.5 \text{ MPa } \sqrt{\text{m}}$, $\Delta T = 1550^\circ\text{C}$).

Outer layer thickness = $2000 \mu\text{m}$. Outer layer/sample thickness = 0.5.

$\text{ZrO}_2 + 35\% \text{Al}_2\text{O}_3$, the first set of observations establishes the lack of matrix cracking in those systems containing at least 50% of zirconia, the residual stress is in fact depleted as the amount of zirconia in outer layers is increased. Matrix cracks could not be detected even at the ends of the beams where edge effects are present; and in fact $\mathcal{R} < \mathcal{R}_c$ is therefore consistent with the absence of matrix cracks.

Further confirmation of the analysis is provided by results of the outer layer without zirconia (pure alumina), in this case $\mathcal{R} = 31$ and profuse cracking is present, in fact $\mathcal{R} \gg \mathcal{R}_c$.

4.2 Crack bifurcation

Vickers indentations were placed into the tensile layer with the intent to explore the crack propagation in our system. Cracks were split after they reach the compressive layer. A simplified model has been developed, see Fig. 7. Assuming that the layers have different thermal expansion coefficients but identical elastic constants as well as thickness, after the propagation the material between the bifurcated crack and the interface is stress free and therefore the residual stress, is given by:

$$\sigma_R^* [1 + h/y] = 2 \sigma_R \quad (6)$$

Where σ_R is the residual stress obtained using eqn (1) while $y/2$ is the crack length propagation in the outer layer (see Fig. 7). Upon loading, the energy release rate is the same at every point of the crack front and if the crack perpendicular to the interface propagates straight into the outer layer, the magnitude is given by:²³

$$\frac{E G}{\sigma_R^2 h} = (1 + y/h) \frac{\pi}{2} \left[\frac{4}{\pi} \sin^{-1} \left(\frac{1}{1 + y/h} \right) - 1 \right]^2 \quad (7)$$

Whereas if the crack after penetrating into the outer layer bifurcates, the energy release rate magnitude is:²³

$$\frac{E G_{\perp}}{\sigma_R^2 h} = \frac{1}{2} [1 - 3y/h] \quad (8)$$

Therefore the strain energy release rate varies linearly with (y/h) in the case of bifurcated cracks whereas there is a different behaviour for the crack that propagates straight into the layer; see Fig. 8. From this figure and from eqns (7) and (8) it is possible to find out that $G \geq G_{\perp}$ at $y/h \approx 0.09$.

Practically the cracks propagate into the outer layers for about 1/20 of ZrO_2 rich layer thickness

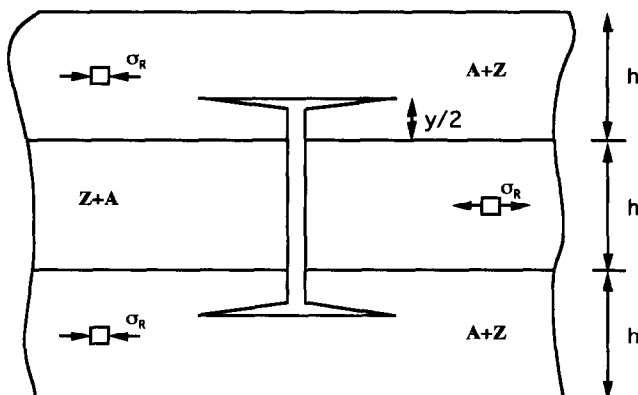


Fig. 7. Schematic example for the crack propagation from the inner layer and subsequent bifurcation.

before bifurcating. To account for this bifurcation phenomenon, the concept of the T -stress²⁴ can also be used. For a mode I crack the T -stress is defined as:

$$\sigma_{ij}(r, \theta) = \frac{K}{\sqrt{2\pi r}} f_{ij}(\theta) + T \delta_{ij} \quad (9)$$

where T is the stress acting parallel to the crack. A crack in an isotropic, homogeneous, brittle solid, selects a trajectory with mode I loading and according with Cotterell and Rice²⁵ a mode I crack is stable if $T < 0$, but unstable if $T > 0$. The T -stress after a crack penetrates into another layer was computed by Suo and Evans, using finite elements.²⁶ From their calculation it appears that conditions exist near the interface with $T > 0$ for value of y/h close to that of our model. The observed bifurcation may be plausibly explained by this effect. To confirm our model we measured the crack penetration in several samples (five for each system) with different inner/outer layer thickness ratio and different compositions. The experimental results are reported in Fig. 9. It is evident that a reasonable agreement exists between the model and experimental results.

4.3. Mechanical properties

Strength was assessed on layered samples with varying outer/inner thickness ratio, with the total

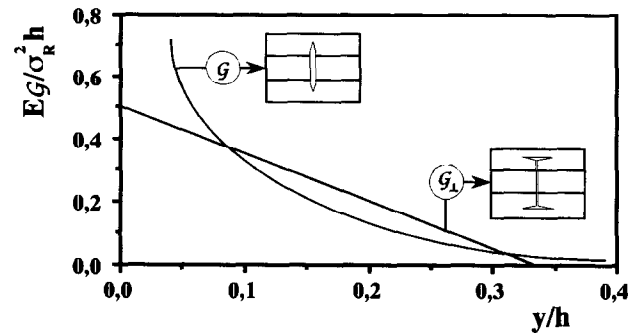


Fig. 8. Trend in the strain energy release rate versus (y/h) for the crack that propagates straight into the layer and for the crack that bifurcates.

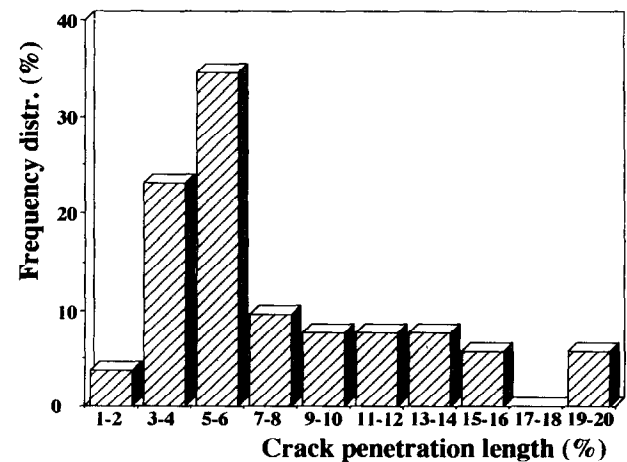


Fig. 9. Experimental results for the crack penetration length before bifurcation.

sample's thickness remaining constant. Strength data are reported in Fig. 10. Over the range of thickness tested, the strength was found to increase with increasing thickness of the inner layer, in fact, for a given total thickness, the magnitude of the predicted surface compressive stress increases with increasing inner layer thickness. The presence of such surface compressive stress makes it more difficult to initiate a failure from flaws in the near surface regions and therefore the material will be less sensitive to degradation caused by surface damage due to contact or abrasion. Fractured samples were examined using scanning electron microscopy, in every case examined the failure was observed to have originated from pre-existing processing flaws. It is evident therefore that much higher strengths should be attainable by improving processing.

5 Conclusions

This work has shown that it is possible to produce, by centrifuging, layered ceramic composites with surface compressive stresses using materials with different thermal expansion coefficients. Although substantial increases in strength have been found, it is clear that better results will occur when processing flaws are reduced. The microstructure obtained when coagulated slurries were sequentially centrifuged was homogeneous. The residual thermal stresses sometimes generate periodic parallel cracks in the tensile layer; a critical non-dimensional parameter \mathcal{R} was used and experimental results confirm that cracks will be suppressed when \mathcal{R} is less than a critical value \mathcal{R}_c .

When a crack propagates from the inner towards the outer layer it deviates just after it penetrates

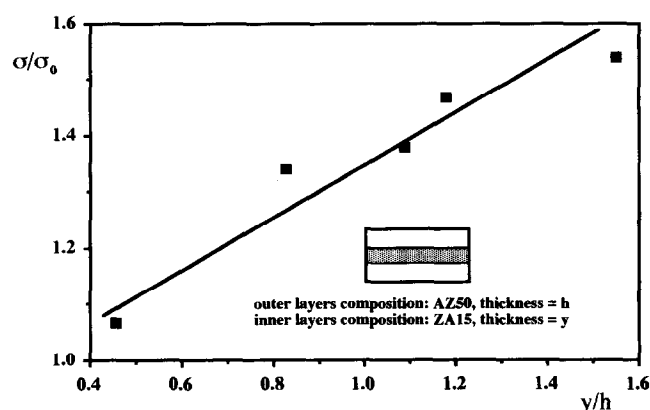


Fig. 10. Bending strength results for a multilayer with fixed layers composition but different thickness ratio (σ_0 is the strength of the outer layer).

the layer under compression. A model was presented taking into account the strain energy release rate of the crack that penetrates straight into the layer compared with that of the crack that bifurcates. The model predicts that bifurcation should occur after the crack propagates for about 1/20 of the outer layer thickness. Experimental results are in good agreement with the model.

References

1. Evans, A. G., *J. Amer. Ceram. Soc.*, **73**(2) (1990) 187–206.
2. Becher, P. F. & Wei, G. C., *J. Amer. Ceram. Soc.*, **67**(12) (1984) C267–9).
3. French, J. D., Chan, H. M., Harmer, M. P. & Miller, G. A., *J. Amer. Ceram. Soc.*, **75**(2) (1992) 418–23.
4. Padture, N. P., *J. Amer. Ceram. Soc.*, **75**(7) (1992) 1870–5.
5. Cook, R. F. & Clarke, D. R., *Acta Metall.*, **36**(3) (1988) 555–62.
6. Masaki, T. & Sinjo, K., *Ceram. Int.*, **13** (1987) 109–12.
7. McMurtry, C. H., Boecker, W. D. G., Seshadri, S. G., Zanghi, J. S. & Garnier, J. E., *Am. Ceram. Soc. Bull.*, **66**(2) (1987) 325–9.
8. Kirschner, H. P., *Strengthening of Ceramics*, Marcel Dekker, New York, 1979.
9. Lange, F. F., *J. Amer. Ceram. Soc.*, **63**(1–2) (1980) 38–40.
10. Virkar, A. V., Huang, J. L. & Cutler, R. A., *J. Amer. Ceram. Soc.*, **70**(3) (1987) 164–70.
11. Chartier, T. & Besson, J. L., *Science of Ceramics*, Vol. 14, ed. D. Taylor, The Institute of Ceramics, UK, 1988, pp. 639–44.
12. Chartier, T., Besson, J. L. & Boch, P., *Advances in Ceramics, Science and Technology of Zirconia III*, Vol. 24, eds S. Somiya, N. Yamamoto, H. Yanagida, Amer. Ceram. Soc., Westerville, Ohio, 1988, pp. 1131–8.
13. Sathyamoorthy, R., Virkar, A. & Cutler, R., *J. Amer. Ceram. Soc.*, **75**(5) (1992) 1136–41.
14. Russo, C. J., Harmer, M. P., Chan, H. M. & Miller, G. A., *J. Amer. Ceram. Soc.*, **75**(12) (1992) 3396–400.
15. Velamakanni, B. V., Chang, J. C., Lange, F. F. & Pearson, D. S., *Langmuir*, **6** (1990) 1323–5.
16. Ho, S. & Suo, Z., *J. Appl. Mech.*, **60** (1993) 890–4.
17. Davidge, R. W. & Green, T. J. *J. Mater. Sci.*, **3** (1968) 629.
18. Ito, Y. M., Rosenblatt, M., Cheng, L. Y., Lange, F. F. & Evans, A. G., *Int. J. Fract.*, **17** (1981) 483.
19. Evans, A. G., *J. Mater. Sci.*, **9** (1974) 1145.
20. Lange, F. F., *Fracture Mechanics of Ceramics*, Vol. 2, Plenum Press, New York, 1976, p. 599.
21. Budiansky, B., Hutchinson, J. W. & Evans, A. G., *J. Mech. Phys. Solids*, **34** (1986) 167.
22. Lu, T. C., Yang, J., Suo, Z., Evans, A. G., Hecht, R. & Mehrabian, R., *Acta Metall. Mater.*, **39**(8) (1991) 1883–90.
23. Tada, H., Paris, P. C. & Irwin, G. R., *The Stress Analysis of Cracks Handbook*, Del Research, St. Louis, MO, 1985.
24. Zak, A. R. & Williams, M. L., *Jnl Appl. Mech.*, **30** (1963) 142–3.
25. Cotterell, B. & Rice, J. R., *Int. J. Fracture*, **16** (1980) 155–69.
26. Ye, T., Suo, Z. & Evans, A. G., *Int. J. Solids and Structures*, in press.